

Microscopic particle-rotor model for the low-lying spectrum of Λ hypernucleiH. Mei,^{1,2} K. Hagino,^{1,3} J. M. Yao,^{1,2} and T. Motoba^{4,5}¹*Department of Physics, Tohoku University, Sendai 980-8578, Japan*²*School of Physical Science and Technology, Southwest University, Chongqing 400715, China*³*Research Center for Electron Photon Science, Tohoku University, 1-2-1 Mikamine, Sendai 982-0826, Japan*⁴*Laboratory of Physics, Osaka Electro-Communications University, Neyagawa 572-8530, Japan*⁵*Yukawa Institute for Theoretical Physics, Kyoto University, Kyoto 606-8502, Japan*

(Received 19 August 2014; revised manuscript received 1 November 2014; published 1 December 2014)

We propose a novel method for low-lying states of hypernuclei based on the particle-rotor model, in which hypernuclear states are constructed by coupling the hyperon to low-lying states of the core nucleus. In contrast to the conventional particle-rotor model, we employ a microscopic approach for the core states; that is, the generator coordinate method (GCM) with the particle number and angular momentum projections. We apply this microscopic particle-rotor model to ${}^9_{\Lambda}\text{Be}$ as an example employing a point-coupling version of the relativistic mean-field Lagrangian. A reasonable agreement with the experimental data for the low-spin spectrum is achieved using the ΛN coupling strengths determined to reproduce the binding energy of the Λ particle.

DOI: [10.1103/PhysRevC.90.064302](https://doi.org/10.1103/PhysRevC.90.064302)

PACS number(s): 21.80.+a, 21.10.Ky, 21.60.Jz, 27.20.+n

I. INTRODUCTION

In the past decade, many high-resolution γ -ray spectroscopy experiments have been carried out for p -shell Λ hypernuclei [1,2]. The measured energy spectra and electric multipole transition strengths in the low-lying states provide rich information on the Λ -nucleon interaction in the nuclear medium and on the impurity effect of the Λ particle on nuclear structure. In this context, several interesting phenomena have been disclosed. One of the most important findings is the appreciable shrinkage of the nuclear core after adding a Λ particle, as compared to the core without Λ [3–6], for which a theoretical prediction has been clearly confirmed in the experiment [7].

The theoretical studies of γ -ray spectroscopy for p -shell hypernuclei have been mainly performed with the cluster model [3,6,8–12] and with the shell model [13–15]. Recently, an *ab initio* method as well as antisymmetrized molecular dynamics (AMD) have also been extended in order to study low-lying states of hypernuclei [16,17]. Most of these models, however, have been limited to light hypernuclei, and it may be difficult to apply them to medium-heavy and heavy hypernuclei.

A self-consistent mean-field approach offers a way to study globally the structure of atomic nuclei as well as hypernuclei from light to heavy systems [18]. In the last decade, self-consistent mean-field models have been applied to study the impurity effect of the Λ particle on the nuclear deformation of p - and sd -shell Λ hypernuclei [19–25]. It has been found that the shape polarization effect of the Λ hyperon is in general not prominent, except for a few exceptions, including ${}^{13}_{\Lambda}\text{C}$, ${}^{23}_{\Lambda}\text{C}$, and ${}^{29,31}_{\Lambda}\text{Si}$ [20].

A drawback of the mean-field approach is that the pure mean-field approximation does not yield a spectrum of nuclei due to the broken symmetries. This can be actually cured by restoring the symmetries by angular momentum and particle number projections. For transitional nuclei, the shape fluctuation effect is also important, and can be taken into account with the generator coordinate method (GCM) or its

approximation, the collective Hamiltonian approach. These schemes are referred to as beyond-mean-field approaches, and have been applied in recent years in order to describe the low-lying spectrum of many even-even nuclei [26].

It has been difficult, however, to extend the beyond-mean-field scheme to odd-mass nuclei. In fact, it has been a long-standing problem in nuclear physics to perform a beyond-mean-field calculation for low-lying states of odd-mass nuclei based on modern energy density functionals. See Ref. [27] for a recent attempt based on the Skyrme energy density functional. One important reason for the difficulty is that the last unpaired nucleon breaks some of the symmetries. Moreover, due to the pairing correlation, many quasiparticle configurations are close in energy and will be strongly mixed with each other. Both of these facts complicate a calculation for low-lying spectra of odd-mass nuclei at the beyond-mean-field level, and have prevented us from quantifying the impurity effect of the Λ particle on the structure of hypernuclei using the mean-field type approaches, even though the first attempt has been undertaken in Ref. [28].

In this paper, we overcome this difficulty by proposing a novel microscopic particle-rotor model for the low-lying states of single- Λ hypernuclei. The novel feature is that we combine the motion of the Λ particle with the core nucleus states, which are described by the state-of-the-art covariant density functional approach; that is, the generator coordinate method (GCM) based on the relativistic mean-field (RMF) approach supplemented with the particle number and the angular momentum projections. We emphasize that with this method a spectrum of hypernuclei is calculated for the first time based on a density functional approach.

The particle-rotor model was firstly proposed by Bohr and Mottelson [29] (see also Ref. [30]), and has recently been applied also to study the structure of odd-mass neutron-rich nuclei, such as ${}^{11}\text{Be}$ [31,32], ${}^{15,17,19}\text{C}$ [33], and ${}^{31}\text{Ne}$ [34]. In this model, the motion of a valence particle is coupled to the rotational motion of a deformed core nucleus, which is usually described by the rigid rotor model. The Pauli principle between the valence nucleon and the nucleons in

the core nucleus is treated approximately. In contrast to this conventional particle-rotor model, in this paper we construct low-lying states of the nuclear core microscopically. That is, we superpose many quadrupole deformed RMF + BCS states, after both the particle-number and the angular-momentum projections are carried out [26]. An idea similar to the microscopic particle-rotor model has recently been employed by Minomo *et al.* in order to describe the structure of the one-neutron halo nucleus ^3He with AMD [35]. We apply this microscopic particle-rotor model to hypernuclei, for which the Pauli principle between the valence Λ particle and the nucleons in the core nucleus is absent. We will demonstrate the applicability of this method by studying the low-lying spectrum of $^9_\Lambda\text{Be}$ as an example.

The paper is organized as follows. In Sec. II, we formulate the microscopic particle rotor model for Λ hypernuclei using the relativistic mean-field Lagrangian. In Sec. III, we apply it to the $^9_\Lambda\text{Be}$ hypernucleus and discuss its low-lying spectrum. We then summarize the paper in Sec. IV.

II. PARTICLE-ROTOR MODEL WITH RELATIVISTIC MEAN-FIELD LAGRANGIAN

We describe a single- Λ hypernucleus as a system in which a Λ hyperon interacts with nucleons inside a nuclear core via scalar and vector contact couplings. The Lagrangian for the single- Λ hypernucleus then reads

$$\mathcal{L} = \mathcal{L}_{\text{free}} + \mathcal{L}_{\text{em}} + \mathcal{L}_{\text{int}}^{NN} + \mathcal{L}_{\text{int}}^{N\Lambda}, \quad (1)$$

where $\mathcal{L}_{\text{free}}$ is the free part of the Lagrangian for the nucleons and the hyperon, \mathcal{L}_{em} is for the photon field which describes the Coulomb interaction between protons, and $\mathcal{L}_{\text{int}}^{NN}$ is the effective strong interaction between nucleons. In this paper, we employ the PC-F1 parameter set for $\mathcal{L}_{\text{int}}^{NN}$ [36], together with a density-independent δ pairing interaction with a smooth cutoff factor [37]. We employ a similar form for the $N\Lambda$ effective interaction term $\mathcal{L}_{\text{int}}^{N\Lambda}$ as in Ref. [38], in which the vector and scalar $N\Lambda$ interaction terms $\hat{V}_V^{N\Lambda}$ and $\hat{V}_S^{N\Lambda}$ are given by

$$\hat{V}_V^{N\Lambda}(\mathbf{r}_\Lambda, \mathbf{r}_N) = \alpha_V^{N\Lambda} \delta(\mathbf{r}_\Lambda - \mathbf{r}_N), \quad (2)$$

$$\hat{V}_S^{N\Lambda}(\mathbf{r}_\Lambda, \mathbf{r}_N) = \alpha_S^{N\Lambda} \gamma_\Lambda^0 \delta(\mathbf{r}_\Lambda - \mathbf{r}_N) \gamma_N^0, \quad (3)$$

respectively. For simplicity, the higher-order coupling terms and the derivative terms in the $N\Lambda$ interaction are not taken into account in the present study.

Based on the idea of particle-rotor model, we expand the total wave function of the core+ Λ particle system with the eigenstates of the core part of the Lagrangian (excluding the $N\Lambda$ term, $\mathcal{L}_{\text{int}}^{N\Lambda}$). That is, we construct the wave function for single- Λ hypernuclei with an even-even nuclear core as

$$\Psi_{IM}(\mathbf{r}_\Lambda, \{\mathbf{r}_N\}) = \sum_{j\ell c} \mathcal{R}_{j\ell c}(\mathbf{r}_\Lambda) \mathcal{F}_{j\ell c}^{IM}(\hat{\mathbf{r}}_\Lambda, \{\mathbf{r}_N\}), \quad (4)$$

where

$$\mathcal{F}_{j\ell c}^{IM}(\hat{\mathbf{r}}_\Lambda, \{\mathbf{r}_N\}) = [\mathcal{Y}_{j\ell}(\hat{\mathbf{r}}_\Lambda) \otimes \Phi_{Ic}(\{\mathbf{r}_N\})]^{(IM)} \quad (5)$$

with \mathbf{r}_Λ and \mathbf{r}_N being the coordinates of the Λ hyperon and the nucleons, respectively. In this equation, I is the total angular momentum and M is its projection onto the z axis for the

whole Λ hypernucleus. $\mathcal{R}_{j\ell c}(\mathbf{r}_\Lambda)$ and $\mathcal{Y}_{j\ell}(\hat{\mathbf{r}}_\Lambda)$ are the four-component radial wave function and the spin-angular wave function for the Λ hyperon, respectively.

In the microscopic particle-rotor model, the wave function for the nuclear core part, $\Phi_{IcM_c}(\{\mathbf{r}_N\})$, is given as a superposition of particle-number and angular-momentum projected RMF + BCS states, $|\varphi(\beta)\rangle$; that is,

$$|\Phi_{IcM_c}\rangle = \sum_{\beta} f_{IcNZ}(\beta) \hat{P}_{M_cK}^{Ic} \hat{P}^N \hat{P}^Z |\varphi(\beta)\rangle, \quad (6)$$

where $\hat{P}_{M_cK}^{Ic}$, \hat{P}^N , \hat{P}^Z are the projection operators onto good numbers of angular momentum, neutrons, and protons, respectively. The mean-field wave functions $|\varphi(\beta)\rangle$ are a set of Slater determinants of quasiparticle states with different quadrupole deformation β . For simplicity, we consider only the axial deformation for the nuclear core and thus the K quantum number is zero in Eq. (6). The weight factor $f_{IcNZ}(\beta)$ is determined by solving the Hill-Wheeler-Griffin equation. We call this scheme a generator coordinate method (GCM) plus particle-number (PN) and one-dimensional angular-momentum (1DAM) projections, or GCM+PN1DAMP. See Ref. [26] for more details on the GCM calculation for the nuclear core states.

Substituting Eq. (4) into the Dirac equation for the whole hypernucleus, $H|\Psi_{IM}\rangle = E_I|\Psi_{IM}\rangle$, where H is the relativistic Hamiltonian corresponding to Eq. (1), one can derive the coupled-channels equations for $\mathcal{R}_{j\ell c}(\mathbf{r}_\Lambda)$, in which the coupling potentials are given in terms of the transition densities from the GCM calculations. The reduced electric quadrupole ($E2$) transition strength can be computed using the $E2$ operator, $\hat{Q}_{2\mu} = \sum_{i \in p} r_i^2 Y_{2\mu}(\hat{\mathbf{r}}_i)$. Notice that we use the bare charge in evaluating the $B(E2)$ strengths, that is, $+e$ for protons and 0 for neutrons and a Λ particle, since our microscopic calculations are in the full configuration space.

III. APPLICATION TO LOW-LYING SPECTRUM OF $^9_\Lambda\text{Be}$

Let us now apply the microscopic particle-rotor model to $^9_\Lambda\text{Be}$ and discuss its low-lying spectrum. To this end, we first carry out the GCM+PN1DAMP calculation for the nuclear core, ^8Be . We generate the mean-field states $|\varphi(\beta)\rangle$ with constrained RMF+BCS calculations with quadrupole deformation. More numerical details can be found in Ref. [26]. In this paper, since we are primarily interested in how the Λ -rotor coupled states emerge in hypernuclei, we here focus our attention onto the ground rotational band and the related hypernuclear states. We thus do not discuss the high-lying states of ^8Be at 16–19 MeV. These states are known to have α -breaking structures [39] and therefore they are out of the present framework, which assumes an axially symmetric shape of ^8Be .

The results of the GCM+PN1DAMP calculation for ^8Be are shown in column (a) in Fig. 1. These energies are in a reasonable agreement with the experimental data shown in column (b) [40], although these are slightly smaller than the observed energies. In view of this, we note that both the 2^+ and 4^+ states are resonance states having large widths in the continuum spectrum, and a proper treatment of boundary conditions is necessary in order to describe them in a consistent

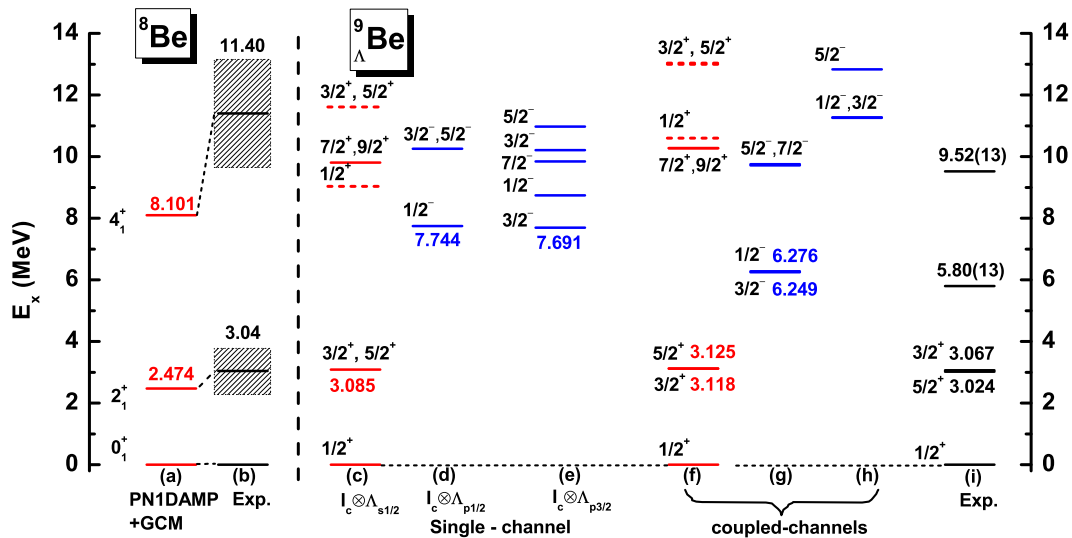


FIG. 1. (Color online) The low-energy excitation spectra of ${}^8\text{Be}$ [columns (a) and (b)] and ${}^9_{\Lambda}\text{Be}$ [columns (c)–(i)]. For ${}^8\text{Be}$, the full GCM+PN1DAMP calculations shown in column (a) are compared with the experimental data taken from Ref. [40]. For ${}^9_{\Lambda}\text{Be}$, columns (c), (d), and (e) show the results of the single-channel calculations for the Λ particle in the $s_{1/2}$, $p_{1/2}$, and $p_{3/2}$ channels, respectively. Columns (f), (g), and (h) show the results of the coupled-channels calculations, which are compared with the experimental data [1,42,43] shown in column (i).

manner. Even though we could reproduce the excitation energy of the 2^+ state by choosing different mesh points in the deformation parameter β in the GCM calculations, here we show the ${}^8\text{Be}$ energy levels calculated with the common set of deformation parameters which better describe the ${}^9_{\Lambda}\text{Be}$.

Let us next discuss the spectrum of ${}^9_{\Lambda}\text{Be}$ constructed using the solutions of the GCM calculations for ${}^8\text{Be}$. To this end, we solve the coupled-channels equations by expanding the radial wave function $\mathcal{R}_{j\ell c}(r_{\Lambda})$ on the basis of eigenfunctions of a spherical harmonic oscillator with 18 major shells. We take the same value for the parameter α_S in the $N\Lambda$ interaction as in Ref. [38] and vary the value of α_V so that the experimental Λ binding energy of ${}^9_{\Lambda}\text{Be}$, $B_{\Lambda}^{\text{(exp)}}({}^9_{\Lambda}\text{Be}) = 6.71 \pm 0.04$ MeV [41], is reproduced with the microscopic particle-rotor model. The resultant values are $\alpha_S^{N\Lambda} = -4.2377 \times 10^{-5}$ MeV $^{-2}$ and $\alpha_V^{N\Lambda} = 1.2756 \times 10^{-5}$ MeV $^{-2}$. The cutoff of the angular momentum for the core states (I_c) is chosen to be 4, which gives well converged results for the low-lying states of ${}^9_{\Lambda}\text{Be}$. We include only the bound core states, that is, the lowest energy state for each value of I_c , even though all the possible states, including continuum states, should be included in principle.

Before we discuss the results of the full coupled-channels calculations, it is useful to investigate the results of single-channel calculations, obtained by ignoring the off-diagonal couplings in the coupled-channels equations. The columns (c), (d), and (e) in Fig. 1 show the results for the Λ particle in the $s_{1/2}$, $p_{1/2}$, and $p_{3/2}$ orbitals, respectively. For the Λ particle in the $s_{1/2}$ orbit, when it is coupled to the core excitation states of 2_1^+ and 4_1^+ , the degenerate $(3/2^+, 5/2^+)$ and $(7/2^+, 9/2^+)$ doublet states in ${}^9_{\Lambda}\text{Be}$ are yielded, respectively. We find that the excitation energies of these two doublet states are slightly larger than those of the corresponding excited states of the core nucleus. This is caused by the fact that the energy gain due to the $N\Lambda$ interaction is larger in the ground state as compared to that in the other states. For the Λ particle in the

$p_{1/2}$ and $p_{3/2}$ orbitals, one obtains the lowest negative parity $1/2^-$ and $3/2^-$ states in ${}^9_{\Lambda}\text{Be}$. The $1/2^-$ state is higher than the $3/2^-$ state by 0.03 MeV, which reflects the size of spin-orbit splitting in the p_{Λ} state of ${}^9_{\Lambda}\text{Be}$. The $1/2_1^-$, $7/2_1^-$, $3/2_2^-$, and $5/2_1^-$ states around 10 MeV in column (e) in Fig. 1 result from the $2^+ \otimes p_{3/2}$ configuration. The order of these states can be understood in terms of the reorientation effect; that is, the diagonal component for the quadrupole term in the coupling potential in the coupled-channels equations. On the other hand, for the $2^+ \otimes p_{1/2}$ configuration, in which the Λ particle in the $p_{1/2}$ orbital is coupled to the 2^+ state of the core nucleus, the quadrupole term does not contribute, and the $3/2^-$ and $5/2^-$ states are degenerate in energy in column (d) in Fig. 1. A more detailed discussion on this characteristic appearance of the multiples will be given in the forthcoming publication [44].

The low-energy spectrum of ${}^9_{\Lambda}\text{Be}$, obtained by mixing these single-channel configurations with the coupled-channels method, is shown in columns (f), (g), and (h) in Fig. 1. The low-lying states are categorized into three rotational bands, whose structures are confirmed by the calculated $B(E2)$ relations. Among these rotational bands, column (g) corresponds to what they called genuine hypernuclear states [3], which are also referred to as the supersymmetric states having $SU(3)$ symmetry $(\lambda\mu) = (50)$ of $s^4 p^5$ shell-model configuration [45]. These states do not have corresponding states in the ordinary nucleus, ${}^9\text{Be}$, because of the Pauli principle of the valence neutron. The calculated spectrum is compared with the available data [1,42,43] shown in column (i) in Fig. 1. One can see that a good agreement with the data is obtained with our calculations. According to our calculations, the measured state with excitation energy of 5.80(13) MeV is actually a mixture of two negative-parity states with $J^{\pi} = 3/2^-$ and $1/2^-$.

Table I lists the values of the probability of the dominant components (with $P_{j\ell c} \geq 0.10$) for a few low-lying states of ${}^9_{\Lambda}\text{Be}$. The unperturbed energies, $E_{\text{ch}}^{(0)}$, obtained by the

TABLE I. The probability P_{jll_c} of the dominant components in the wave function for low-lying states of ${}^9_\Lambda\text{Be}$ obtained by the microscopic particle-rotor model. Only those components which have P_{jll_c} larger than 0.1 are shown. E is the energy of each state obtained by solving the coupled-channels equations, while $E_{1\text{ch}}^{(0)}$ is the unperturbed energy obtained with the single-channel calculations. The energies are listed in units of MeV.

I^π	E	$(lj) \otimes I_c$	P_{jll_c}	$E_{1\text{ch}}^{(0)}$	I^π	E	$(lj) \otimes I_c$	P_{jll_c}	$E_{1\text{ch}}^{(0)}$
$1/2_1^+$	0.000	$s_{1/2} \otimes 0^+$	0.928	0.000	$1/2_2^+$	10.603	$s_{1/2} \otimes 0^+$	0.995	9.035
$3/2_1^+$	3.118	$s_{1/2} \otimes 2^+$	0.919	3.085	$3/2_2^+$	13.034	$d_{3/2} \otimes 0^+$	0.841	11.467
$5/2_1^+$	3.125	$s_{1/2} \otimes 2^+$	0.919	3.085	$5/2_2^+$	12.999	$s_{1/2} \otimes 2^+$	0.131	11.610
$7/2_1^+$	10.267	$s_{1/2} \otimes 4^+$	0.894	9.807	$7/2_2^+$	15.510	$d_{5/2} \otimes 0^+$	0.845	11.450
$9/2_1^+$	10.281	$s_{1/2} \otimes 4^+$	0.894	9.807	$9/2_2^+$	15.483	$s_{1/2} \otimes 2^+$	0.125	11.610
$1/2_1^-$	6.276	$p_{1/2} \otimes 0^+$	0.516	7.744	$7/2_2^+$	15.510	$d_{3/2} \otimes 2^+$	0.833	13.804
$3/2_1^-$	6.249	$p_{3/2} \otimes 2^+$	0.445	8.741	$9/2_2^+$	15.483	$d_{5/2} \otimes 2^+$	0.112	14.124
$5/2_1^-$	9.756	$p_{3/2} \otimes 0^+$	0.524	7.691	$1/2_2^-$	11.271	$p_{1/2} \otimes 0^+$	0.575	7.744
$7/2_1^-$	9.717	$p_{3/2} \otimes 2^+$	0.220	10.212	$3/2_2^-$	11.258	$p_{3/2} \otimes 2^+$	0.419	8.741
		$p_{1/2} \otimes 2^+$	0.217	10.259	$5/2_2^-$	12.835	$p_{3/2} \otimes 0^+$	0.568	7.691
		$p_{1/2} \otimes 2^+$	0.625	10.259	$7/2_2^-$	15.729	$p_{3/2} \otimes 2^+$	0.220	10.212
		$p_{3/2} \otimes 2^+$	0.186	10.978			$p_{1/2} \otimes 2^+$	0.206	10.259
		$p_{3/2} \otimes 4^+$	0.150	14.935			$p_{3/2} \otimes 2^+$	0.769	10.978
		$p_{3/2} \otimes 2^+$	0.813	9.842			$p_{1/2} \otimes 2^+$	0.226	10.259
		$p_{1/2} \otimes 4^+$	0.100	15.926			$p_{1/2} \otimes 2^+$	0.603	9.842
							$p_{1/2} \otimes 4^+$	0.216	15.926
							$p_{3/2} \otimes 4^+$	0.157	16.215

single-channel calculations are also shown for each component. One can see that the positive-parity states in the ground state rotational band are almost pure $I_c^+ \otimes \Lambda_{s_{1/2}}$ states, while there are appreciable configuration mixings for the negative-parity states as well as the positive-parity states in the excited band. For instance, for the first negative-parity state, $1/2_1^-$, there is a strong mixing between the $0^+ \otimes \Lambda_{p_{1/2}}$ and the $2^+ \otimes \Lambda_{p_{3/2}}$ configurations with almost equal weights. It is remarkable that the present calculation reconfirms an interesting prediction of the cluster model; that is, the strong coupling of a hyperon to the collective rotation is realized when the Λ is in the p orbit [3]. It is interesting to notice that the values of P_{jll_c} obtained in the present calculations are similar to those with the cluster model calculations shown in Fig. 1 of Ref. [3]. This large admixture is caused by the fact that the unperturbed energies, $E_{1\text{ch}}^{(0)}$, are similar to each other for these configurations due to the reorientation effect. We also remark that in the second positive parity states (I_2^+) the Λ_d state is admixed appreciably, while in the second negative parity states (I_2^-) the wave functions have the ‘‘out-of-phase’’ nature in comparison with the corresponding first negative parity states (I_1^-).

Table II shows the calculated $E2$ transition strengths for low-lying states of ${}^8\text{Be}$ and ${}^9_\Lambda\text{Be}$. The calculated $E2$ transition strengths for $2^+ \rightarrow 0^+$ and $4^+ \rightarrow 2^+$ in ${}^8\text{Be}$ are $25.0 e^2\text{fm}^4$ and $47.3 e^2\text{fm}^4$, respectively, which are slightly larger than the values $22.4 e^2\text{fm}^4$ and $39.3 e^2\text{fm}^4$ [3] (as well as $19.6 e^2\text{fm}^4$ and $30.0 e^2\text{fm}^4$ [5]) obtained with the cluster model calculations. Both of these calculations overestimate the recently measured $B(E2 : 4^+ \rightarrow 2^+)$ value, $21 \pm 2.3 e^2\text{fm}^4$ [46], by a factor of about 2. For ${}^9_\Lambda\text{Be}$, the experimental upper limit for the

lifetime of 0.1 ps has been deduced for the first $3/2^+$ and $5/2^+$ states [42], which corresponds to the $B(E2)$ value larger than $29.07 e^2\text{fm}^4$ [42,43]. The present calculation slightly underestimates this value (see Table II), possibly due to a limitation of the model space mentioned below.

As has been pointed out in Ref. [3], each state in ${}^9_\Lambda\text{Be}$ can be classified in terms of the total orbital angular momentum L , which couples to the spin 1/2 of the Λ particle to form the total angular momentum I . In order to remove the trivial factor due to the angular momentum coupling for spin 1/2 and see more clearly the impurity effect of Λ particle on nuclear collectivity, we follow Ref. [3] and compute the $cB(E2)$ value defined as

$$cB(E2 : L_i \rightarrow L_f) \equiv \hat{L}_i^{-2} \hat{I}_f^{-2} \left\{ \begin{matrix} L_f & I_f & 1/2 \\ I_i & L_i & 2 \end{matrix} \right\}^{-2} B(E2 : I_i \rightarrow I_f), \quad (7)$$

TABLE II. The calculated $E2$ transition strengths (in units of $e^2\text{fm}^4$) for low-lying states of ${}^8\text{Be}$ and ${}^9_\Lambda\text{Be}$. $cB(E2 : L_i \rightarrow L_f)$ is defined by Eq. (7), where L is the total orbital angular momentum.

${}^8\text{Be}$		${}^9_\Lambda\text{Be}$			
$I_i^\pi \rightarrow I_f^\pi$	$B(E2)$	$I_i^\pi \rightarrow I_f^\pi$	$(L_i^\pi \rightarrow L_f^\pi)$	$B(E2)$	$cB(E2)$
$2_1^+ \rightarrow 0_1^+$	24.99	$3/2_1^+ \rightarrow 1/2_1^+$	$(2^+ \rightarrow 0^+)$	22.55	22.55
		$5/2_1^+ \rightarrow 1/2_1^+$	$(2^+ \rightarrow 0^+)$	22.57	22.57
$4_1^+ \rightarrow 2_1^+$	47.28	$7/2_1^+ \rightarrow 3/2_1^+$	$(4^+ \rightarrow 2^+)$	37.43	41.58
		$9/2_1^+ \rightarrow 5/2_1^+$	$(4^+ \rightarrow 2^+)$	41.55	41.55
		$7/2_1^+ \rightarrow 5/2_1^+$	$(4^+ \rightarrow 2^+)$	4.152	41.52
		$5/2_1^- \rightarrow 1/2_1^-$	$(3^- \rightarrow 1^-)$	13.14	16.90
		$7/2_1^- \rightarrow 3/2_1^-$	$(3^- \rightarrow 1^-)$	17.15	17.15

where $\hat{I} \equiv \sqrt{2I+1}$. The impurity effect of Λ particle on ${}^8\text{Be}$ can be discussed by comparing the $B(E2)$ values in ${}^8\text{Be}$ and the $cB(E2)$ values in ${}^9_{\Lambda}\text{Be}$ in Table II. One can see that the $E2$ strengths are slightly decreased due to the shrinkage effect of Λ hyperon.

The degree of reduction in $B(E2)$ with the present model is much smaller than the results of cluster model calculations [3,5,47]. Also, in our calculation, the energy of the 2^+ state increases significantly by adding a Λ particle, whereas the experimental data as well as the cluster model calculations indicate that the energy shift is negligibly small [3,5,47] (see Fig. 1). These discrepancies between the present calculation and the cluster model calculations would be due to the effects of higher members of the core excited states, which are not included in present calculations. However, with the current implementation of GCM, we have a limitation in constructing the wave functions for the nonresonant core states (that is, the second and the third 0^+ , 2^+ , and 4^+ states), which extend up to large values of deformation parameter β . For this reason, we did not obtain reasonable results for the hypernuclear states above $5/2_1^+$ when we included the higher members of the core states.

IV. SUMMARY

We have proposed a novel method for a low-lying spectrum of hypernuclei based on a mean-field type approach. Whereas the pure mean-field approximation does not yield a spectrum due to the broken rotational symmetry, we employed a beyond-relativistic mean-field approach by carrying out the angular momentum and the particle number projections as well as the configuration mixing with the generator coordinate method. In this novel method, the beyond-mean-field approach is applied to low-lying states of the core nucleus, to which the Λ hyperon couples in the wave function of hypernuclei, and thus we call it the microscopic particle-rotor model. We emphasize that this is the first calculation for a spectrum of hypernuclei based on a density functional approach. By applying the microscopic particle-rotor model to ${}^9_{\Lambda}\text{Be}$, a reasonable agreement with the experimental data of low-spin spectrum has been achieved without introducing any adjustable parameters, except for the

$N\Lambda$ coupling strengths, which were determined to reproduce the Λ binding energy. More details on the microscopic particle model, including also a comparison with a nonrelativistic approach, will be introduced in the forthcoming publication [44].

In this paper, since our main focus was on a proposal of a novel method for spectra of hypernuclei, we have assumed the axial deformation for the core nucleus ${}^8\text{Be}$ and taken into account only the ground rotational band. An obvious extension of our method is to take into account the triaxial deformation of the core nucleus. One interesting candidate for this is ${}^{25}_{\Lambda}\text{Mg}$, for which the triaxial degree of freedom has been shown to be important in the core nucleus ${}^{24}\text{Mg}$ [22,26,48]. A treatment of high-lying collective states in the core nucleus will also be an important issue.

Another point which we would like to make is that the microscopic particle-rotor model proposed in this paper is much beyond the picture of the conventional particle-rotor model, in the sense that the core excited states are given by the full microscopic beyond-mean-field calculations, where the collective motions of both rotations and vibrations, as well as their couplings, are taken into account automatically with the angular momentum projection and GCM. It will be interesting to apply systematically the present method to many hypernuclei and to study a transition in the low-lying spectrum from a vibrational to a rotational characters. An application of our method to a production of hypernuclei is another interesting problem. To this end, one would need to apply the present method consistently also to ordinary nuclei with an odd number of nucleons, for which a treatment of the Pauli principle would make it more complicated as compared to hypernuclei studied in this paper.

ACKNOWLEDGMENTS

This work was supported in part by the Tohoku University Focused Research Project ‘‘Understanding the origins for matters in universe,’’ JSPS KAKENHI Grant No. 26400263, the National Natural Science Foundation of China under Grants No. 11305134 and No. 11105111, and the Fundamental Research Funds for the Central Universities (XDJK2010B007 and XDJK2013C028).

-
- [1] O. Hashimoto and H. Tamura, *Part. Nucl. Phys.* **57**, 564 (2006).
 - [2] H. Tamura, *Int. J. Mod. Phys. A* **24**, 2101 (2009).
 - [3] T. Motoba, H. Bandō, and K. Ikeda, *Prog. Theor. Phys.* **70**, 189 (1983).
 - [4] T. Motoba, H. Bandō, K. Ikeda, and T. Yamada, *Prog. Theor. Phys. Suppl.* **81**, 42 (1985).
 - [5] Yu You-wen, T. Motoba, and H. Bandō, *Prog. Theor. Phys.* **76**, 861 (1986).
 - [6] E. Hiyama, M. Kamimura, K. Miyazaki, and T. Motoba, *Phys. Rev. C* **59**, 2351 (1999).
 - [7] K. Tanida *et al.*, *Phys. Rev. Lett.* **86**, 1982 (2001).
 - [8] E. Cravo, A. C. Fonseca, and Y. Koike, *Phys. Rev. C* **66**, 014001 (2002).
 - [9] V. M. Suslov, I. Filikhin, and B. Vlahovic, *J. Phys. G: Nucl. Part. Phys.* **30**, 513 (2004); I. N. Filikhin, V. M. Suslov, and B. Vlahovic, *Phys. At. Nucl.* **76**, 355 (2013).
 - [10] M. Shoeb and Sonika, *Phys. Rev. C* **79**, 054321 (2009).
 - [11] H. Bando, T. Motoba and J. Žofka, *Int. J. Mod. Phys. A* **5**, 4021 (1990).
 - [12] E. Hiyama, Y. Kino, and M. Kamimura, *Prog. Part. Nucl. Phys.* **51**, 223 (2003).
 - [13] R. H. Dalitz and A. Gal, *Ann. Phys. (N.Y.)* **116**, 167 (1978).
 - [14] A. Gal, J. M. Soper, and R. H. Dalitz, *Ann. Phys. (N.Y.)* **63**, 53 (1971).
 - [15] D. J. Millener, *Nucl. Phys. A* **804**, 84 (2008); **914**, 109 (2013).
 - [16] R. Wirth, D. Gazda, P. Navratil, A. Calic, J. Langhammer, and R. Roth, *Phys. Rev. Lett.* **113**, 192502 (2014).
 - [17] M. Isaka, M. Kimura, A. Doté, and A. Ohnishi, *Phys. Rev. C* **83**, 044323 (2011); **83**, 054304 (2011).
 - [18] M. Bender, P.-H. Heenen, and P.-G. Reinhard, *Rev. Mod. Phys.* **75**, 121 (2003).

- [19] X.-R. Zhou, H.-J. Schulze, H. Sagawa, C.-X. Wu, and E.-G. Zhao, *Phys. Rev. C* **76**, 034312 (2007).
- [20] M. T. Win and K. Hagino, *Phys. Rev. C* **78**, 054311 (2008).
- [21] H.-J. Schulze, M. T. Win, K. Hagino, and H. S. Sagawa, *Prog. Theo. Phys.* **123**, 569 (2010).
- [22] Myaing Thi Win, K. Hagino, and T. Koike, *Phys. Rev. C* **83**, 014301 (2011).
- [23] B.-N. Lu, E.-G. Zhao, and S.-G. Zhou, *Phys. Rev. C* **84**, 014328 (2011).
- [24] A. Li, E. Hiyama, X.-R. Zhou, and H. Sagawa, *Phys. Rev. C* **87**, 014333 (2013).
- [25] B.-N. Lu, E. Hiyama, H. Sagawa, and S.-G. Zhou, *Phys. Rev. C* **89**, 044307 (2014).
- [26] J. M. Yao, J. Meng, P. Ring, and D. Vretenar, *Phys. Rev. C* **81**, 044311 (2010); J. M. Yao, H. Mei, H. Chen, J. Meng, P. Ring, and D. Vretenar, *ibid.* **83**, 014308 (2011); J. M. Yao, H. Mei, and Z. P. Li, *Phys. Lett. B* **723**, 459 (2013); J. M. Yao, K. Hagino, Z. P. Li, J. Meng, and P. Ring, *Phys. Rev. C* **89**, 054306 (2014).
- [27] B. Bally, B. Avez, M. Bender, and P.-H. Heenen, *Int. J. Mod. Phys. E* **21**, 01250026 (2012); *Phys. Rev. Lett.* **113**, 162501 (2014).
- [28] J. M. Yao *et al.*, *Nucl. Phys. A* **868**, 12 (2011).
- [29] A. Bohr and B. R. Mottelson, *Nuclear Structure Vol. II* (Benjamin, Reading, MA, 1975).
- [30] P. Ring and P. Schuck, *The Nuclear Many Body Problem* (Springer-Verlag, New York, 1980).
- [31] H. Esbensen, B. A. Brown, and H. Sagawa, *Phys. Rev. C* **51**, 1274 (1995).
- [32] F. M. Nunes, I. J. Thompson, and R. C. Johnson, *Nucl. Phys. A* **596**, 171 (1996).
- [33] T. Tarutina and M. S. Hussein, *Phys. Rev. C* **70**, 034603 (2004).
- [34] Y. Urata, K. Hagino, and H. Sagawa, *Phys. Rev. C* **83**, 041303(R) (2011).
- [35] K. Minomo, T. Sumi, M. Kimura, K. Ogata, Y. R. Shimizu, and M. Yahiro, *Phys. Rev. Lett.* **108**, 052503 (2012).
- [36] T. Burvenich, D. G. Madland, J. A. Maruhn, and P.-G. Reinhard, *Phys. Rev. C* **65**, 044308 (2002).
- [37] S. J. Krieger *et al.*, *Nucl. Phys. A* **517**, 275 (1990).
- [38] Y. Tanimura and K. Hagino, *Phys. Rev. C* **85**, 014306 (2012).
- [39] T. Yamada, K. Ikeda, H. Bando, and T. Motoba, *Phys. Rev. C* **38**, 854 (1988).
- [40] V. M. Datar, S. Kumar, D. R. Chakrabarty, V. Nanal, E. T. Mirgule, A. Mitra, and H. H. Oza, *Phys. Rev. Lett.* **94**, 122502 (2005).
- [41] A. Gal, *Advances in Nucl. Phys.* **8**, 1 (1975).
- [42] H. Tamura *et al.*, *Nucl. Phys. A* **754**, 58c (2005).
- [43] H. Akikawa *et al.*, *Phys. Rev. Lett.* **88**, 082501 (2002).
- [44] H. Mei, K. Hagino, J. M. Yao, and T. Motoba (unpublished).
- [45] R. H. Dalitz and A. Gal, *Phys. Rev. Lett.* **36**, 362 (1976).
- [46] V. M. Datar *et al.*, *Phys. Rev. Lett.* **111**, 062502 (2013).
- [47] K. Hagino and T. Koike, *Phys. Rev. C* **84**, 064325 (2011).
- [48] S. W. Robinson and R. D. Bent, *Phys. Rev.* **168**, 1266 (1968).